J Nanostruct Chem (2014) 4:95–101
DOI 10.1007/s40097-014-0118-x

ORIGINAL

A novel zinc(II) macrocycle-based synthesis of pure ZnO nanoparticles

V. Pushpanathan · D. Suresh Kumar

Received: 14 April 2014 / Accepted: 23 June 2014 / Published online: 30 July 2014

Abstract Dinuclear zinc(II) complex of the 18-membered tetraiminediphenol macrocycle has been synthesized by Schiff base condensation of 2,6-diformyl-4-methylphenol and 1,2-diaminobenzene in the presence of zinc(II) template. The obtained complex has been characterized by the spectroscopic techniques and mass spectrometry. The complex exhibits high thermal stability and forms ZnO nanoparticles on thermal decomposition. The diffraction peaks in the X-Ray diffraction spectra indicated that the complexes are crystalline. The surface morphology has been investigated by scanning electron microscopy. Energy dispersive X-ray analysis shows the chemical purity and stoichiometry of the ZnO nanoparticles. The BET surface area of ZnO nanoparticles has been found. The transmission electron microscopy result shows spherical shaped ZnO nanoparticles with the size of 20 nm. Quantum confinement effects are clearly revealed in UV–Vis spectroscopy technique.

Keywords 2,6–Diformyl–4–methylphenol · ZnO nanoparticles · Tetraiminediphenol macrocycle · Zinc complex · Surface morphology

Introduction

Zinc oxide is a well-known semiconductor material with a wide band gap (3.37 eV) and a large exciton binding energy (60 meV) at room temperature [1]. ZnO nanoparticles have been extensively studied over the past decades because of their fascinating electrical [2], mechanical [3], optical [4], and piezoelectric properties [5]. ZnO nanoparticles have a wide range of applications such as gas sensors [6], dye-sensitized solar cells [7], ultra violet photodetectors [8], UV lasers [9], photocatalysts [10], piezoelectric transducers [11], and for biomedical applications [12]. They have been synthesized by various methods such as chemical vapor deposition [13], sol–gel method [14], low-temperature wet chemical methods [15], electrochemical deposition [16], laser ablation [17], pulsed laser deposition [18], thermal decomposition [19], spray pyrolysis [20], radiofrequency magnetron sputtering [21], and hydrothermal method [22]. The main purpose of each method is to prevent the crystallite agglomeration, control the particle shape, size, and crystal phase of ZnO nanoparticles. We know that ZnO nanoparticles with certain morphology and size could be obtained using suitable surfactant and solvent. Moreover, it requires suitable conditions to stabilize the nanoparticles. However, most of the methods have been found to be expensive, polluting, and time consuming. Therefore, it still remains an extremely difficult challenge to find a simple and mild synthetic route to synthesize well-controlled ZnO nanoparticles.

It has been reported [23–26] that thermal decomposition method is an efficient, simple, one-step, solvent-free approach to generate ZnO nanoparticles. As compared to other methods [27–30], it is much faster, pollution free, and economical. However, the use of macrocyclic complexes as precursors for the preparation of metal oxide nanomaterial's such as ZnO using thermal decomposition has not yet been investigated. Hence we made an attempt to synthesize ZnO nanoparticles using Zn(II) complex of tetraiminediphenol macrocycle as precursor for the first time.

V. Pushpanathan · D. Suresh Kumar (✉)
Supramolecular Research Laboratory, Department of Chemistry, Loyola College, Chennai 600 034, Tamilnadu, India
e-mail: drdsklc@gmail.com

Results and discussion

In the earlier work we have reported [31–34] the efficient synthesis of a series of tetraiminediphenol macrocyclic ligands by the Schiff base condensation of diformyls with diamines in the presence of lanthanide(III) metal ions as their complexes by template method and have reported their thermal stability. The stability of the complexes has been influenced by the rigidity of the ligand backbone. The results clearly reveal that tetraiminediphenol macrocyclic framework formed by the condensation of 2,6-diformyl-4-substituted phenols with 1,2-diaminobenzene could provide the required rigidity and, therefore, has the greater ability to stabilize the central metal ion. As part of our continuing interest to synthesize metal complexes of macrocyclic ligands, we have synthesized zinc(II) complex with the similar ligand framework. We also have made an attempt to synthesize the metal oxide nanoparticles using this metal complex. Therefore, the dinuclear zinc(II) complex of tetraiminediphenol macrocycle has been synthesized by the modified procedure of Garcia et al. [35] where the [2+2] template condensation is carried out between 2,6-diformyl-4-methylphenol and 1,2-diaminobenzene in the presence of zinc(II) nitrate hexahydrate in methanol.

From the results of elemental analysis, molar conductivity measurements, and spectroscopic studies, the stoichiometry of the complex has been deduced as $[Zn_2L](NO_3)_2$, similar to the complex synthesized by Garcia et al. This macrocyclic entity has N_4O_2 donor framework from four imine and two phenolate groups and, therefore, stabilizes comfortably the two zinc ions in their +2 oxidation state. The structure of the dinuclear zinc(II) complex of the 18-membered tetraiminediphenol macrocycle is shown in Fig. 1.

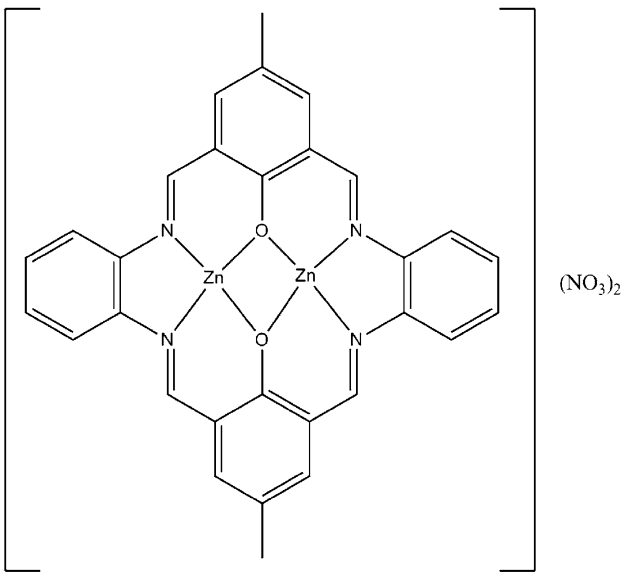

Fig. 1 Structure of the complex $[Zn_2L](NO_3)_2$

Thermal studies

The thermal behavior of $[Zn_2L](NO_3)_2$ has been studied by TG/DTA analysis. The complex shows initial weight loss of about 17.9 % in the temperature range of 400–430 °C which corresponds to the loss of two ionic nitrates (calculated value is 17.17 %). The macrocyclic entity which remained unchanged up to 430 °C undergoes a gradual weight loss beyond 430 °C associated with the thermal decomposition of macrocyclic entity. The resultant mass of the decomposition product is in conformity with the mass of pure ZnO [36] which could be nanocrystalline. Moreover, it is understood that the complex exhibits relatively high thermal stability and controls the size of the nanoparticles formed. The thermogram of the complex is shown in Fig. 2. Therefore, on thermal decomposition of the complex for 4 h at 500 °C, spherical ZnO nanoparticles with good separation are produced. This method of preparation shows the macrocyclic complex may be suitable precursors for the preparation of ZnO nanoparticles.

Phase study

The X-Ray diffraction (XRD) pattern of ZnO nanoparticles is shown in Fig. 3, which confirms that the nanoparticles are wurtzite structured ZnO with nominal cell constants of $a = b = 3.249$ Å and $c = 5.206$ Å (JCPDS 65–3411). No diffraction peaks from impurity phases are detected in this study. These results indicate that only single-phase ZnO is present [37]. Further observation revealed that ZnO nanoparticles have sharp peaks with broad width, indicating high crystallinity with small particle size [38, 39]. The average particle size can be calculated from the Scherrer's formula [40]:

$$D = \frac{K\lambda}{\beta \mathrm{Cos}\theta}$$

where D is the average crystallite size, λ is the wavelength of the X-ray radiation (Cu Kα radiation, 0.15406 nm), β is the full width at half maximum (FWHM), θ is the diffraction angle, and K is the Scherrer constant (0.9). Here, the (100), (002), and (101) reflection peaks of ZnO were used to calculate the average particle size. From the calculation, it is clear that the particles are in the range 20–30 nm.

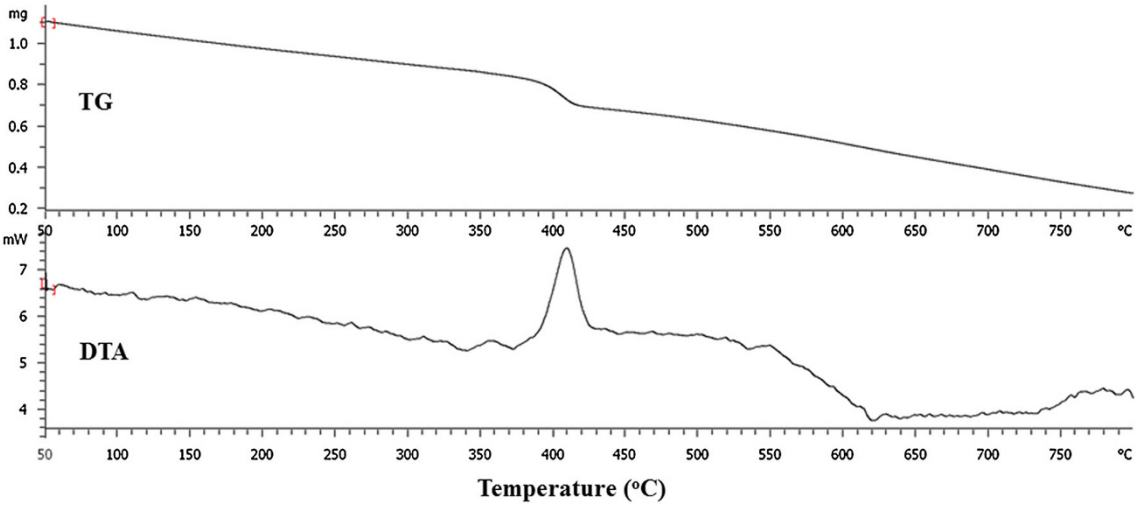

Fig. 2 TG and DTA curves of the complex $[Zn_2L](NO_3)_2$

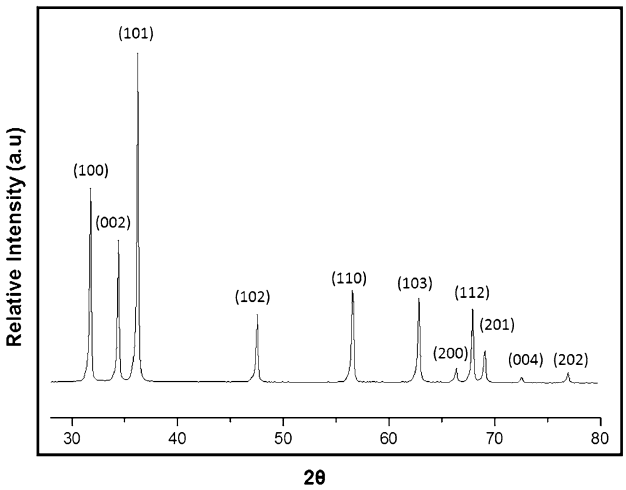

Fig. 3 XRD pattern of ZnO nanoparticles

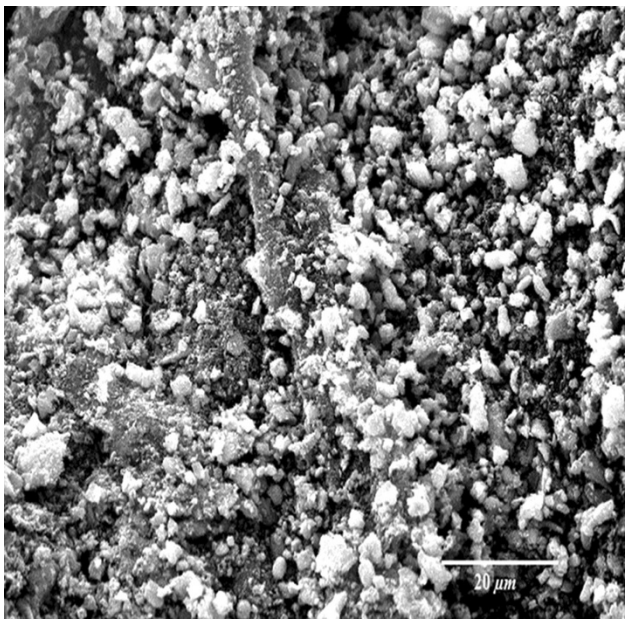

Fig. 4 SEM image of ZnO nanoparticles

Morphology study

The morphology of the ZnO nanoparticles produced by the thermal decomposition of macrocyclic complex at 500 °C was investigated by scanning electron microscopy (SEM). The SEM image shows that the particles are small and spherical shaped ZnO nanostructures with good separation as shown in Fig. 4. The energy dispersive X-ray (EDS) spectrum of the ZnO nanoparticles is shown in Fig. 5. Peaks associated with Zn and O atoms are only observed in this EDS spectrum, which confirms that the nanoparticles are purely ZnO. The detailed structure of ZnO nanoparticles has been characterized by transmission electron microscope (TEM) and selected area electron diffraction (SAED). Fig. 6 shows TEM analysis of the ZnO nanoparticles. The TEM image shows spherical shaped ZnO nanoparticles with the size of 20 nm. The size of the nanoparticles from the TEM micrograph agrees with the XRD result. The inset is its SAED analysis which confirms that the nanoparticles are wurtzite with single crystalline nature. The measured BET surface area of ZnO nanoparticles has been found to be 42.32 m^2/g. It shows that nanoparticles prepared by this method are small, spherical, more crystalline, of higher purity, and also have large specific surface areas [41, 42], which could enhance the catalytic activity [43, 44].

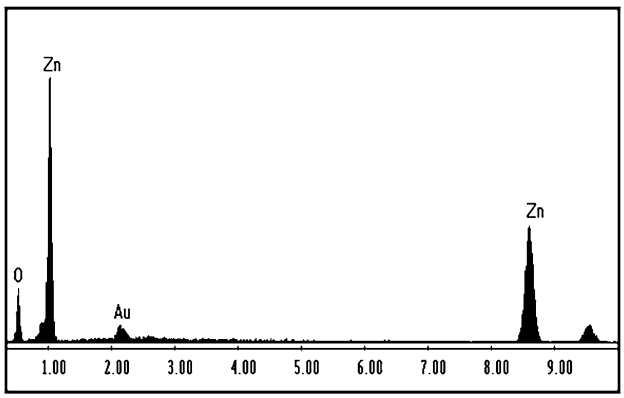

Fig. 5 EDS spectrum of ZnO nanoparticles

UV–Visible diffuse reflectance spectral study

The UV–Visible absorbance spectrum of the ZnO nanoparticles at room temperature is shown in Fig. 7. The absorption spectrum shows a well-defined exciton band at 366 nm and significant blue shift of about 7 nm with respect to the bulk exciton absorption (373 nm) [45]. It is clear that the absorption edge shifts to the lower wavelength or higher energy with decreasing size of the nanoparticle. This blue shift in the absorption spectrum is due to the quantum confinement effect of these small size ZnO nanoparticles [46].

The optical band gap of ZnO nanoparticles is estimated by extrapolation of the linear relationship between $(\alpha h\upsilon)^2$ and $h\upsilon$ according to the equation [47].

$$\alpha h\upsilon = A\,(h\upsilon - Eg)^{1/2}$$

where α is the absorption coefficient, $h\upsilon$ is the photon energy, E_g is the optical band gap, and A is a constant. A Tauc plot of $(\alpha h\upsilon)^2$ versus $h\upsilon$ is shown in Fig. 8, by extrapolating the graph to X-axis to find the band gap of the nanoparticles. The band gap is found to be 3.38 eV which is slightly higher than that of bulk ZnO (3.37 eV). The increase in energy gap may be due to decrease in size of the nanoparticles.

Experimental

Materials

2,6–Diformyl–4–methylphenol was synthesized according to the literature method [48]. 1,2–Diaminobenzene (Sigma-Aldrich) and zinc(II) nitrate hexahydrate (Merck, India) were purchased and used as such. All solvents were of analytical grade and were purified [49] prior to use.

Analytical and physical measurements

Microanalytical (C, H, N) data were obtained with a FLASH EA 1112 Series CHNS Analyzer. The IR spectra (with KBr pellets) were recorded in the range of 400–4000 cm^{-1} on a JASCO FT/IR-5300 FT-IR spectrometer. Diffuse reflectance and near-IR absorption spectra were recorded on a UV-3600 Shimadzu UV–Vis-NIR spectrophotometer. ^1H NMR spectra were recorded on a Bruker AVANCE III 400 MHz (AV400) multinuclear NMR spectrometer at 400 MHz and 100 MHz, respectively. ESI mass spectra were obtained on a LCMS-2010A Shimadzu spectrometer. The TG–DTA analyses were conducted on a TA Q600 SDT instrument at a standard heating rate of 10 °C min^{-1} between room temperature (30 °C) and 1000 °C under a dynamic nitrogen

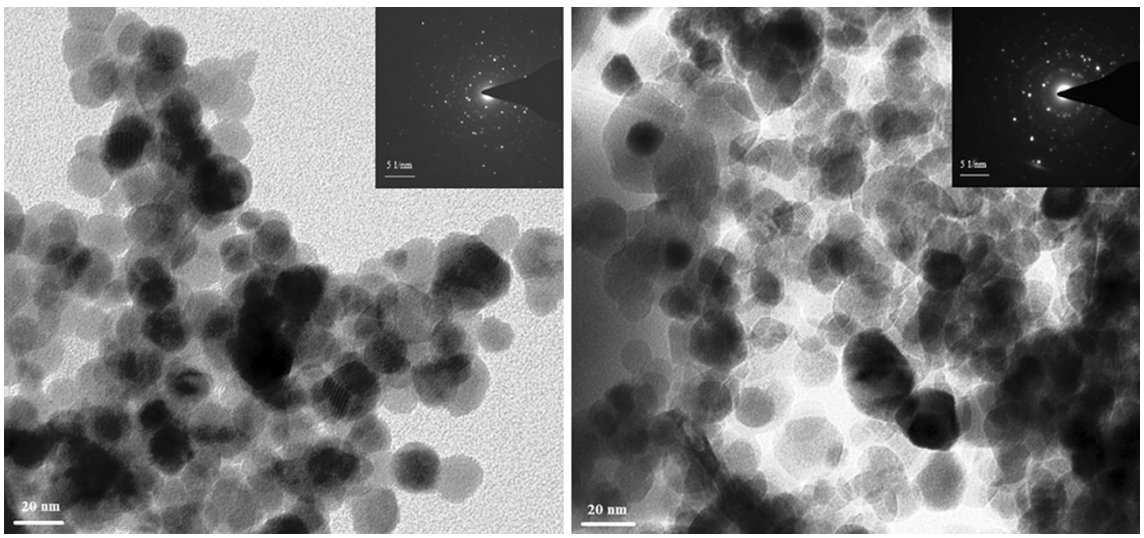

Fig. 6 TEM images of ZnO nanoparticles. Inset shows its SAED pattern

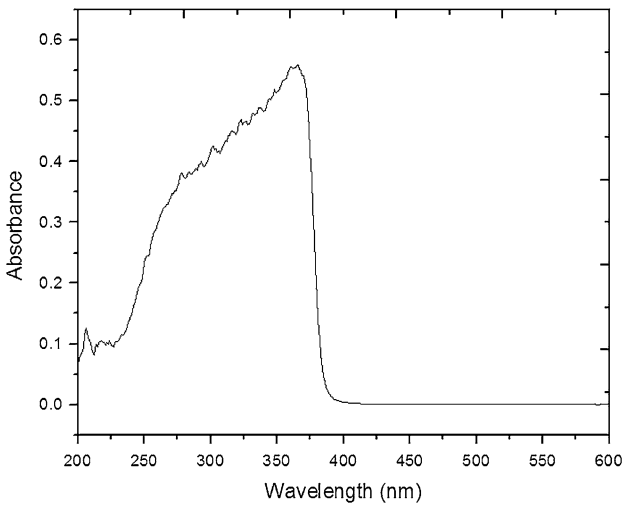

Fig. 7 UV-Visible spectrum of ZnO nanoparticles

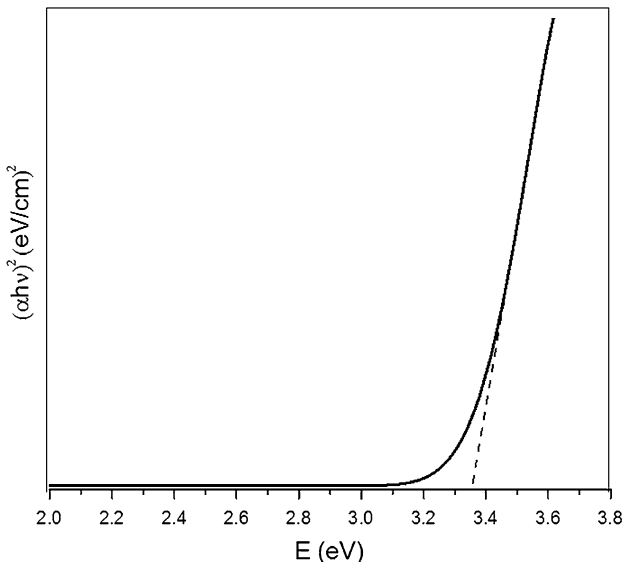

Fig. 8 Tauc plot of $(\alpha h\upsilon)^2$ versus $h\upsilon$

atmosphere. Powder X-ray diffraction patterns were recorded on a Bruker D8-Advance diffractometer using graphite monochromated $CuK_{\alpha 1}$ (1.5406 Å) and $K_{\alpha 2}$ (1.5444 Å) radiations. The SEM and EDS (energy dispersive X-ray spectrometry) analyses were performed on Philips XL-30 Scanning Electron Microscope operating at 20 kV. Specimens for analysis were prepared by dusting the compounds on carbon tape. The TEM analyses were conducted on FEI technai G^2 20 STEM with a 200 kV acceleration voltage. TEM specimens were prepared on carbon-coated copper grids with 200 meshes. Samples were suspended in suitable solvents and ultra sonicated for 1–2 min. Measurement of BET surface area was carried out using Quantachrome Autosorb iQ BET surface area analyzer.

Synthesis of zinc(II) complex, $[Zn_2L](NO_3)_2$

A solution of 2,6-diformyl-4-methylphenol (0.164 g, 1 mmol) and zinc(II) nitrate hexahydrate (0.297 g, 1 mmol) in methanol (50 mL) was refluxed for 30 min. Another solution of 1,2-diaminobenzene (0.108 g, 1 mmol) in methanol was added to the above hot solution drop by drop for 15 min. The resultant orange solution was refluxed for 3 h with stirring. The brick red solid product that separated out was filtered, washed repeatedly with methanol followed by chloroform, and dried under vacuum over anhydrous calcium chloride. Yield: 35 %. Anal. Calcd for $C_{30}H_{22}N_6O_8Zn_2$: C, 49.68; H, 3.06 N, 11.59; Zn, 18.04. Found: C, 49.56; H, 3.12; N, 11.45; Zn, 18.12 %. UV–Vis (DMSO), λ_{max}: 296 (13756), 361 (9574), 416 (10331), 450 (6975) nm ($dm^3\ mol^{-1}\ cm^{-1}$). FT–IR (cm^{-1}) in KBr: 1616 ($\nu_{C=N}$), 1534 ($\nu_{C=C}$), 1298 (ν_{C-O}), 761 (ν_{C-H}), 547 (ν_{Zn-N}). ^1H NMR ($DMSOd_6$, ppm): 2.33 (s, 6H, $-CH_3$), 6.84–7.28 (m, 12H, aromatic), 8.58 (s, 4H, –CH = N). Λ_M (DMSO): 34.61 $ohm^{-1}\ cm^2\ mol^{-1}$. ESI MS (*m/z*): 723 $(M-H)^+$.

Synthesis of zinc oxide nanoparticles

The brick red dinuclear zinc(II) macrocyclic complex, $[Zn_2L](NO_3)_2$, was taken in a porcelain crucible and heated in an electric furnace at the rate of 10 °C min^{-1} from room temperature (30 °C) to 500 °C in air atmosphere. The calcination of the complex is done for 4 h by selecting the temperature from the TG–DTA data. The decomposed white product generated from the macrocyclic complex was cooled to room temperature and collected for characterization.

Conclusion

ZnO nanoparticles with wurtzite structure have been synthesized by a simple, single-step method of thermal decomposition with zinc(II) complex of tetraiminediphenol macrocycle. From the results of XRD, SEM, TEM, and BET, the ZnO nanoparticles are spherical shaped single crystalline with the size of 20 nm and also have large specific surface areas. The blue shift in the absorption spectrum is due to the quantum confinement effect of these nano size ZnO nanoparticles. These studies show the macrocyclic complex may be suitable precursors for the preparation of nanomaterials with reduced size.

Acknowledgments The author (V. Pushpanathan) is thankful to Dr. Samar Kumar Das and UGC-NRC, School of Chemistry, University of Hyderabad, for the instrumentation facility.

References

1. Wan, Q., Li, Q.H., Chen, Y.J., Wang, T.H., He, X.L., Li, J.P., Lin, C.L.: Fabrication and ethanol sensing characteristics of ZnO nanowire gas sensors. Appl. Phys. Lett. **84**, 3654 (2004)
2. Garcia, M.A., Merino, J.M., Pinel, E.F., Quesada, A., de la Venta, J., Ruiz, M.L., Gonzalez, G.R., Castro, P., Crespo, J., Llopis, J.M., Gonzalez-Calbet, Hernando, A.: Magnetic properties of ZnO nanoparticles. Nano Lett. **7**, 1489 (2007)
3. Chernikov, A., Horst, S., Waitz, T., Tiemann, M., Chatterjee, S.: Photoluminescence properties of ordered mesoporous ZnO. J. Phys. Chem. C **115**, 1375 (2011)
4. Zhao, Q., Xie, T., Peng, L., Lin, Y., Wang, P., Peng, L., Wang, D.: Wang, Size- and orientation-dependent photovoltaic properties of ZnO nanorods. J. Phys. Chem. C **111**, 17136 (2007)
5. Scrymgeour, D.A., Hsu, J.W.P.: Correlated piezoelectric and electrical properties in individual ZnO nanorods. Nano Lett. **8**, 2204 (2008)
6. Spencer, M.J.S., Yarovsky, I.: ZnO nanostructures for gas sensing: Interaction of NO_2, NO, O, and N with the ZnO (1010) surface. J. Phys. Chem. C **114**, 10881 (2010)
7. Anta, J.A., Guillen, E., Tena-Zaera, R.: ZnO-based dye-sensitized solar cells. J. Phys. Chem. C **116**, 11413 (2012)
8. Jin, Y., Wang, J., Sun, B., Blakesley, J.C., Greenham, N.C.: Solution-processed ultraviolet photodetectors based on colloidal ZnO nanoparticles. Nano Lett. **8**, 1649 (2008)
9. Sakai, T., Nakano, I., Shimo, M., Takamori, N., Takahashi, A.: Thermal direct mastering using deep UV laser. Jpn. J. Appl. Phys. **45**, 1407 (2006)
10. Mclaren, A., Valdes-Solis, T., Li, G., Tsang, S.C.: Shape and size effects of ZnO nanocrystals on photocatalytic activity. J. Am. Chem. Soc. **131**, 12540 (2009)
11. Lu, M.P., Song, J., Lu, M.Y., Chen, M.T., Gao, Y., Chen, L.J., Wang, Z.L.: Piezoelectric nanogenerator using p-type ZnO nanowire arrays. Nano Lett. **9**, 1223 (2009)
12. Xiong, H.M.: ZnO nanoparticles applied to bioimaging and drug delivery. Adv. Mater. **25**, 5329 (2013)
13. Zhang, B.P., Binh, N.T., Wakatsuki, K., Segawa, Y., Yamada, Y., Usami, N., Kawasaki, M., Koinuma, H.: Formation of highly aligned ZnO tubes on sapphire (0001) substrates. Appl. Phys. Lett. **84**, 4098 (2004)
14. Tokumoto, M.S., Pulcinelli, S.H., Santilli, C.V., Briois, V.: Catalysis and temperature dependence on the formation of ZnO nanoparticles and of zinc acetate derivatives prepared by the sol-gel route. J. Phys. Chem. B **107**, 568 (2003)
15. Richardson, J.J., Lange, F.F.: Controlling low temperature aqueous synthesis of ZnO. 1. Thermodynamic analysis. Cryst. Growth Des. **9**, 2570 (2009)
16. Lu, X.H., Wang, D., Li, G.R., Su, C.Y., Kuang, D.B., Tong, Y.X.: Controllable electrochemical synthesis of hierarchical ZnO nanostructures on FTO glass. J. Phys. Chem. C **113**, 13574 (2009)
17. Usui, H., Shimizu, Y., Sasaki, T., Koshizaki, N.: Photoluminescence of ZnO nanoparticles prepared by laser ablation in different surfactant solutions. J. Phys. Chem. B **109**, 120 (2005)
18. Premkumar, T., Zhou, Y.S., Lu, Y.F., Baskar, K.: Optical and field-emission properties of ZnO nanostructures deposited using high-pressure pulsed laser deposition. ACS Appl. Mater. Interfaces **2**, 2863 (2010)
19. Hosseinifard, M., Hashemi, L., Amani, V., Morsali, A.: Characterization of pure phase Zn(II) oxide nanoparticles via thermal decomposition of two zinc(II) complexes of the 6,6′-dimethyl-2,2′-bipyridine ligand. J. Struct. Chem. **54**, 396 (2013)
20. Height, M.J., Madler, L., Pratsinis, S.E., Krumeich, F.: Nanorods of ZnO made by flame spray pyrolysis. Chem. Mater. **18**, 572 (2006)
21. Youssef, S., Combette, P., Podlecki, J., Al Asmar, R., Foucaran, A.: Structural and optical characterization of ZnO thin films deposited by reactive rf magnetron sputtering. Cryst Growth Des. **9**, 1088 (2009)
22. Xu, X., Wu, M., Asoro, M., Ferreira, P.J., Fan, D.L.: One-step hydrothermal synthesis of comb-like ZnO nanostructures. Cryst. Growth Des. **12**, 4829 (2012)
23. Aghabeygi, S., Bigdeli, F., Morsali, A.: Synthesis and characterization of zinc(II) oxide nanoparticles by thermal decomposition of two zinc(II) nitrite coordination polymer precursors. J. Inorg. Organomet. Polym. **22**, 526 (2012)
24. Bagabas, A.A., Apblett, A.W., Shemsi, A.M., Seddigi, Z.S.: X-ray crystal structure, spectroscopic characterization, and thermal chemistry of trans-diaqua-bis-(2-hydroxyiminopropionato-N,O) zinc(II), trans-$\{(H_2O)_2[H_3CC(=NOH)COO)]_2Zn\}$ – A precursor for nano-crystalline zincite. Main Group Chem. **7**, 65 (2008)
25. Niasari, M.S., Davar, F., Mazaheri, M.: Preparation of ZnO nanoparticles from [bis(acetylacetonato)zinc(II)]–oleylamine complex by thermal decomposition. Mater. Lett. **2008**, 62 (1890)
26. Khanpour, M., Morsali, A.: Synthesis and characterization of one-dimensional zinc(II) coordination polymers as precursors for preparation of ZnO nanoparticles *via* thermal decomposition. J. Inorg. Organomet. Polym. **21**, 360 (2011)
27. Yang, Y., Li, X.F., Chen, J.B., Chen, H.L., Bao, X.M.: ZnO nanoparticles prepared by thermal decomposition of β-cyclodextrin coated zinc acetate. Chem. Phys. Lett. **373**, 22 (2003)
28. Yang, Y., Chen, H., Zhao, B., Bao, X.: Size control of ZnO nanoparticles via thermal decomposition of zinc acetate coated on organic additives. J. Cryst. Growth **263**, 447 (2004)
29. Wang, R.C., Tsai, C.C.: Efficient synthesis of ZnO nanoparticles, nanowalls, and nanowires by thermal decomposition of zinc acetate at a low temperature. Appl. Phys. A **94**, 241 (2009)
30. Hossienifard, M., Hashemi, L., Amani, V., Kalateh, K., Morsali, A.: Synthesis and characterization of ZnO nanoparticles via thermal decomposition of two zinc (II) supramolecular compounds. J. Inorg. Organomet. Polym. **21**, 527 (2011)
31. Kumar, D.S., Alexander, V.: Synthesis of lanthanide(III) complexes of chloro- and bromo substituted 18-membered tetraaza macrocycles. Polyhedron **18**, 1561 (1999)
32. Kumar, D.S., Alexander, V.: Macrocyclic complexes of lanthanides in identical ligand frameworks part 1. Synthesis of lanthanide(III) and yttrium(III) complexes of an 18-membered dioxatetraaza macrocycle. Inorg. Chim. Acta **238**, 63 (1995)
33. Kumar, D.S., Aruna, V.A.J., Alexander, V.: Synthesis of homodinuclear lanthanide(III) complexes of 24-membered tetraaza and 34-membered octaaza Schiff base macrocycles. Polyhedron **18**, 3123 (1999)
34. James, S., Kumar, D.S., Alexander, V.: Synthesis of lanthanide(III) complexes of 20-membered octaaza and hexaaza schiff-base macrocycles. J. Chem. Soc. Dalton Trans. **11**, 1773 (1999)
35. Garcia, V.P., Yazigi, D.V., Cabrera, A., Galvez, P.V., Arriagada, M., Leon, D.R., Pizarro, N., Zanocco, A., Spodine, E.: Optical properties of binuclear zinc (II) macrocyclic complexes derived

from 4-methyl-2,6-diformylphenol and 1,2-diaminobenzene. Polyhedron **28**, 2335 (2009)
36. Wang, L., Muhammed, M.: Synthesis of zinc oxide nanoparticles with controlled morphology. J. Mater. Chem. **9**, 2871 (1999)
37. Zhu, Y.F., Zhou, G.H., Ding, H.Y., Liu, A.H., Lin, Y.B., Li, N.L.: Controllable synthesis of hierarchical ZnO nanostructures *via* a chemical route. Physica E **42**, 2460 (2010)
38. Zhang, Z., Liu, R., Zhao, M., Qian, Y.: Synthesis of metal and metal oxide nanocrystallines by pyrolysis of metal complex. Mater. Chem. Phys. **71**, 161 (2001)
39. Rekha, K., Nirmala, M., Nair, M.G., Anukaliani, A.: Structural, optical, photocatalytic and antibacterial activity of zinc oxide and manganese doped zinc oxide nanoparticles. Phys. B **405**, 3180 (2010)
40. Scherrer, P.: Nachr ges wiss Gottingen. Math. Phys. **2**, 98 (1918)
41. Chen, J., Li, J., Li, J., Xiao, G., Yang, X.: Large-scale syntheses of uniform ZnO nanorods and ethanol gas sensors application. J. Alloys Compd. **509**, 740 (2011)
42. Vigneshwaran, N., Kumar, S., Kathe, A.A., Varadarajan, P.V., Prasad, V.: Functional finishing of cotton fabrics using zinc oxide–soluble starch nanocomposites. Nanotechnology **17**, 5087 (2006)
43. Pernicone, N.: Catalysis at the nanoscale level. Cattech **7**, 196 (2003)
44. Polarz, S., Orlov, A.V., Schuth, F., Lu, A.H.: Preparation of high-surface-area zinc oxide with ordered porosity, different pore sizes, and nanocrystalline walls. Chem. Eur. J. **13**, 592 (2007)
45. Haase, M., Weller, H., Henglein, A.: Photochemistry and radiation chemistry of colloidal semiconductors. 23. Electron storage on zinc oxide particles and size quantization. J. Phys. Chem. **92**, 482 (1988)
46. Koch, U., Fojtik, A., Weller, H., Henglein, A.: Photochemistry of semiconductor colloids. Preparation of extremely small ZnO particles, fluorescence phenomena and size quantization effects. Chem. Phys. Lett. **122**, 507 (1985)
47. Caglar, M., Ilican, S., Caglar, Y.: Influence of dopant concentration on the optical properties of ZnO: In films by sol–gel method. Thin Solid Films **517**, 5023 (2009)
48. Gagne, R.R., Spiro, C.L., Smith, T.J., Hamann, C.A., Thies, W.R., Shiemke, A.K.: The synthesis, redox properties, and ligand binding of heterobinuclear transition-metal macrocyclic ligand complexes. Measurement of an apparent delocalization energy in a mixed-valent copper(I) copper(II) complex. J. Am. Chem. Soc. **103**, 4073 (1981)
49. Furniss, B.S., Hanna ford, A.J., Rogers, V., Smith, P.W.G., Tatchell, A.R.: 4th edn. (1978)